



The role of carbonic anhydrase in the recovery of skeletal muscle from anoxia

Krzysztof Wroblewski, Simon Spalhoff, Un-Jin Zimmerman, Robert L. Post, Joseph W. Sanger and Robert E. Forster

Journal of Applied Physiology 99:488-498, 2005. First published Mar 31, 2005;
doi:10.1152/jappphysiol.01409.2004

You might find this additional information useful...

This article cites 46 articles, 23 of which you can access free at:

<http://jap.physiology.org/cgi/content/full/99/2/488#BIBL>

Updated information and services including high-resolution figures, can be found at:

<http://jap.physiology.org/cgi/content/full/99/2/488>

Additional material and information about *Journal of Applied Physiology* can be found at:

<http://www.the-aps.org/publications/jappl>

This information is current as of August 20, 2005 .

The role of carbonic anhydrase in the recovery of skeletal muscle from anoxia

Krzysztof Wroblewski,^{1,2} Simon Spalthoff,³ Un-Jin Zimmerman,^{2,4}
Robert L. Post,^{2,4} Joseph W. Sanger,^{2,5} and Robert E. Forster^{2,4}

¹Department of Radiology, ²School of Medicine, University of Pennsylvania, Philadelphia, Pennsylvania;

³Zentrum Physiologie, Medizinische Hochschule Hannover, Hannover, Germany; and Departments of

⁴Physiology and ⁵Cell and Developmental Biology, University of Pennsylvania, Philadelphia, Pennsylvania

Submitted 22 December 2004; accepted in final form 29 March 2005

Wroblewski, Krzysztof, Simon Spalthoff, Un-Jin Zimmerman, Robert L. Post, Joseph W. Sanger, and Robert E. Forster. The role of carbonic anhydrase in the recovery of skeletal muscle from anoxia. *J Appl Physiol* 99: 488–498, 2005. First published March 31, 2005; doi:10.1152/jappphysiol.01409.2004.—To investigate the role of carbonic anhydrase in the recovery of skeletal muscle from anoxia, pH and cell phosphates were measured by ³¹P-nuclear magnetic resonance in superfused newborn rabbit myotubes and cultured mouse soleus cells (H-2K^b-ts a58) after ~2–3.5 h without superfusion. In control studies, pH and phosphocreatine fell and P_i rose during anoxia and recovered within <10 min after reperfusion began. A carbonic anhydrase inhibitor, acetazolamide, and dimethylamiloride, an inhibitor of the Na⁺/H⁺ antiporter NHE1, delayed the recoveries of pH, phosphocreatine, and P_i for >10 min, but the rate of recovery, once initiated, was unchanged. In the presence of the inhibitors, after reperfusion started, the pH did not rise immediately, despite a large inwardly directed HCO₃⁻ gradient, suggesting that HCO₃⁻ movement was unimportant in acid elimination. Lactate, measured by its methyl protons, rose during anoxia and did not fall after 1 h of reperfusion and could not have eliminated protons by cotransport. We conclude that NHE1 is the major exporter of protons by skeletal muscle in recovery from a period of anoxia and that it is essential for functioning carbonic anhydrase to be attached to NHE1 to activate it. The mechanism of late recovery of pH could be the mobilization of another proton transporter or removal of the inhibition of the Na⁺/H⁺ antiporter. Inhibition of carbonic anhydrase in skeletal muscle retards acid removal and modifies muscle metabolism significantly after anoxia.

skeletal muscle cells; pH; NMR; acetazolamide; dimethylamiloride

WE HYPOTHESIZED THAT ONE (or more) of the four carbonic anhydrase (CA) (EC 4.2.1.1) isozymes in skeletal muscle (13) are required to remove the acid produced by heavy exercise or anoxia. Kowalchuk et al. (24) have administered a sulfonamide CA inhibitor, acetazolamide (AZ), to human subjects and measured the rate of recovery of intracellular pH of an arm muscle after exercise by ³¹P-NMR. The onset of the realkalization of muscle pH was delayed by the drug, but this did not necessarily implicate muscle CA, because erythrocyte CA would have also been inhibited, which would have reduced the rate of acid (CO₂) removal from muscle by blood. We attempted to inhibit muscle CA separately from erythrocyte CA with a membrane-permeable and highly active sulfonamide inhibitor, ethoxzolamide, but this approach was unsuccessful. We report here studies by NMR of the rate of recovery of pH

and phosphorus metabolites of isolated, suspended skeletal muscle cells (33) from acidosis. The cells were in suspension rather than attached to a flat substrate (48) to pack a larger volume of cells into the NMR tube. We used anoxia to produce acidosis rather than NH₃ export to mimic and exaggerate the partial deoxygenation that occurs in working muscle. We chose to study neonatal rabbit myocytes cultured on gelatin beads (26), which develop into mature skeletal muscle myotubes with well-characterized contractile elements. We also studied a skeletal muscle cell line, H-2K^b-ts a58 (H-2K).

METHODS

The experimental procedures were carried out under protocols approved by the Institutional Animal Care Committee of the University of Pennsylvania. The first preparation was a primary culture of newborn rabbit muscle myocytes cultured under 95% O₂ and 5% CO₂ with 100- to 300- μ m cross-linked gelatin beads at 37°C in DMEM (GIBCO 11885) containing 10% newborn calf serum and 1% penicillin/streptomycin. The myocytes attach themselves to the beads, fuse, and in ~3 wk form myotubes that contain the myosin of mature striated muscle cells, predominantly fast-type glycolytic (Fig. 1A), and can be seen to contract rhythmically. The second preparation was a myoblast cell line (Fig. 1B) prepared from H-2K mouse soleus muscle, provided to us by T. A. Partridge (32), and cultured in the same medium as the rabbit myocytes plus 2% chicken embryo extract and 10,000 units of interferon. From 0.25 to 1.25 ml of the packed cells (200–500 \times 10⁶ cells) were separated from the culture flasks with 0.25% trypsin and embedded in agarose beads (agarose type VII-low gelling temperature, Sigma A-4018) (Fig. 1C) in each experiment (5, 8). The perfusion system (Fig. 2) consisted of a 10-mm precision diameter glass NMR sample tube to hold the cells in the spectrometer, to which were attached an inflow line and two outflow lines, consisting of 4 m of 0.88-mm inner diameter polyvinyl chloride tubing to deliver and remove perfusate. A shorter line was available to withdraw outflowing samples of perfusate by hand. A porous (35- μ m pores) 3-mm-thick polyethylene filter disk held the cells in place. A capillary tube containing a water solution of methylene diphosphonic acid (MDP) provided a phosphate standard. The perfusate was impelled by a four-headed peristaltic pump outside the magnetic field.

The perfusate consisted of DMEM (GIBCO 11971), which originally contained, in addition to other lesser components, 110 mM NaCl, 44 mM NaHCO₃, 25 mM D-glucose, no phosphate, and no pyruvate, to which was added 10% newborn calf serum and 1% penicillin/streptomycin. It was sparged at 40°C with filtered 95% O₂–5% CO₂ gas. However, the perfusate unavoidably lost more O₂ than CO₂ in passing through the pump and 4 m of plastic tubing so that it had a Pco₂ of 45 Torr, a Po₂ of ~485 Torr, a pH of 7.5, and a

Address for reprint requests and other correspondence: R. E. Forster, Dept. of Physiology, A201 Richards Bldg., School of Medicine, Univ. of Pennsylvania, Philadelphia, PA 19104–6085 (E-mail: forster@mail.med.upenn.edu).

The costs of publication of this article were defrayed in part by the payment of page charges. The article must therefore be hereby marked “advertisement” in accordance with 18 U.S.C. Section 1734 solely to indicate this fact.

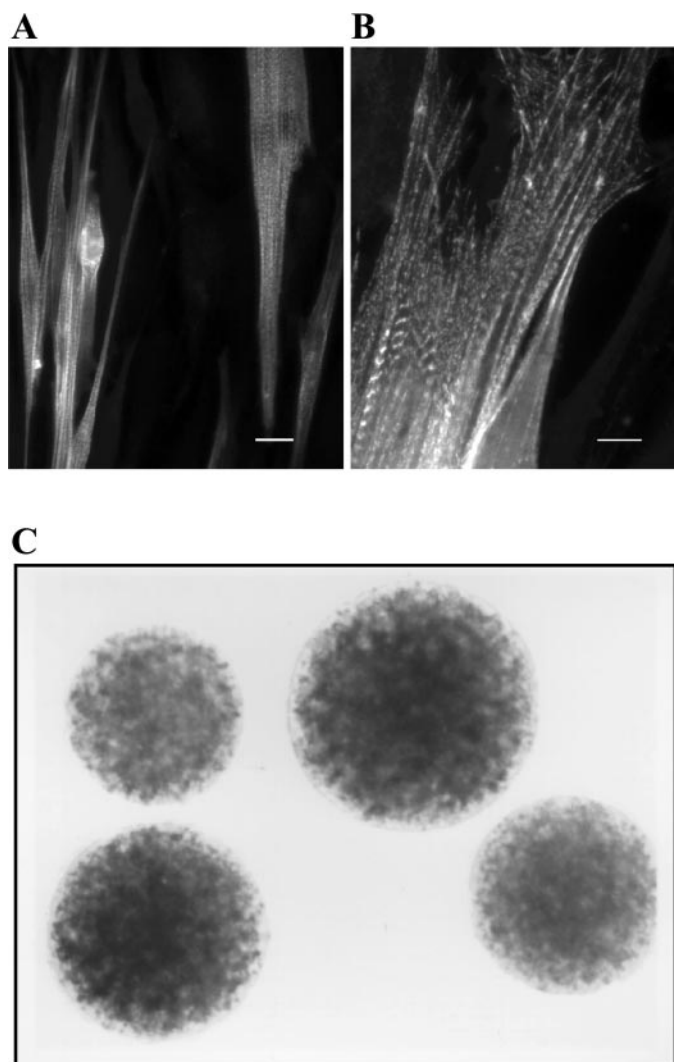


Fig. 1. Photographs of myotubes grown on flat surfaces (*A* and *B*) and embedded within beads (*C*). *A*: neonatal rabbit skeletal muscle myotubes. *B*: myotube formed from the fusion of H-2K^b-ts a58 (H-2K) myoblasts. Both preparations were stained with sarcomeric α -actinin antibodies. Bars = 10 μ m. *C*: agarose beads with embedded H-2K cells. The diameter of the *right* lower bead was 500 μ m.

HCO₃⁻ of 36 mM when it reached the cells. The volume of the tubing from roller pump to sample was 2.48 ml, and that of the sample of beads plus entrapped fluid was ~2.5 ml. With a perfusion flow rate of 2 ml/min, the perfusion fluid in the system should have been replaced four times within a spectrum accumulation time of 10 min. We verified this experimentally by washout of a phosphate solution from the sample tube.

The NMR spectra were obtained on a Bruker AMX-500 spectrometer at the phosphorus resonance frequency, 202.5 MHz, using a Bruker selective ³¹P/¹H 10-mm probe. The temperature of the sample tube was stabilized at 311K (38°C), which was checked with a nonmagnetic temperature probe. To avoid radio-frequency heating and the Nuclear Overhauser Effect, which would affect signal intensities, the spectra were obtained without proton decoupling. Spectra were usually obtained with a 10-min acquisition time (400 spectra), a 45° pulse, and a relaxation delay of 1.5 s and were processed using standard Bruker software. The T₁ values of the phosphate compounds were <1 s (37), and the peak areas were corrected by the equation of Hsieh and Balaban (16). A line broadening of 20 Hz and Lorentzian curve fitting were applied to obtain NMR signal areas. The signal

from the MDP standard, which was totally visible to the radio-frequency coil, was used to calculate the absolute amount of phosphate represented by each peak. To calculate the concentration of a phosphate compound in the cells, we assumed a standard ATP concentration in the stabilization period of 4.3 μ mol/ml and divided this into the micromoles of ATP in the cells during the stabilization period determined by NMR to obtain the volume of cells in the NMR tube. The concentration of any molecular species was its amount divided by the cell volume. We obtained the average value of 4.3 mM ATP in the cells by measuring the amount of P_i in four samples of superfused H-2K cells in the NMR tube when 1) the perfusate contained no phosphate, 2) when it contained 0.9 mM P_i, and 3) when the cells and polyethylene disk were removed from the tube, and it was filled with the perfusate containing 0.9 mM phosphate. From these data, one can also calculate the volume of cells in each experiment, which was between 0.1 and 0.6 ml (average 0.3 ml).

The amount of PCr in the cells was too small to measure accurately, so 24 mM creatine was added to the culture medium at least 2 days before an experiment and to the perfusate. When creatine was omitted from the culture medium, the concentration of PCr was less than that of ATP. Daly and Seifter (7) showed that muscle cells take up creatine slowly by one or more saturable transporters sensitive to external Na⁺ concentration, which can raise cellular creatine by an order of magnitude. The creatine forms phosphocreatine (PCr) by the action of creatine kinase, consuming ATP in the process (43). pH was calculated from the chemical shift of P_i from the MDP standard using the equation of Kemp et al. (23), adding the chemical shift between MDP and PCr determined in phosphate solution. This equation is valid for calculation of pH values between 5.5 and 8.0. Lactate measurements were done on a Bruker AMX-300 spectrometer at the proton resonance frequency, 300 MHz, using a 10 mM broadband probe with a proton decoupling coil. The double quantum sequence described by Jouvensal et al. (19) was used to eliminate a contribution from lipid to the lactate signal, which signal was confirmed with lactate solution.

CA activity was determined by the changing pH method of Henry (15) at 4°C. Bovine CA (95% protein, Sigma) was used as a standard.

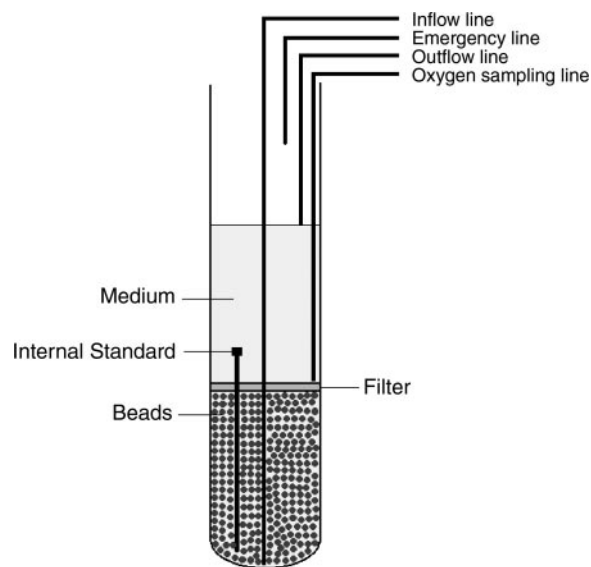


Fig. 2. Diagram of the glass tube with its plastic tubing connections that fit inside the magnet and contain the cell carriers. Perfusate flows in through the “inflow” line, passes upward through the cell, through the plastic disk, until it is drawn out in the “outflow” line, set to maintain 6 ml of perfusate above the plastic filter disk. The sampling line is placed just above the plastic disk to collect perfusate just as it leaves the disk. The emergency line is placed above the fluid level to prevent the fluid level from rising higher if the outflow line becomes overloaded. This means that air is continuously flowing into the gas phase above the fluid.

We analyzed both cell types for CA activity and found 0.030 μM CA in a preparation of myotubes and 0.068 μM in H-2K cells. By comparison with the human red blood cell, in which the reversible CO_2 reactions are accelerated $\sim 17,000$ times at body temperature (17), the concentrations of enzymes in the cells studied would be expected to accelerate the reactions ~ 40 – 60 times.

We were unable to calculate O_2 and CO_2 exchanges of the perfused cells by the Fick principle because of the small differences in concentration of O_2 and CO_2 and of pH between the inflowing and outflowing samples of perfusate. As an alternative, we measured O_2 consumption in two aliquots of H-2K cells at 35°C in a oxygen electrode chamber. Their total volume was calculated from a microscopic count in a hemocytometer and a measured cell diameter (10.7 μm). The included fluid volume in lightly packed cells was 0.31 of the total. The average consumption rate was 0.006 $\text{ml O}_2 \cdot \text{ml cells}^{-1} \cdot \text{min}^{-1}$, the same in the presence or absence of 0.1 mM AZ. This is a very low value but comparable to the published value of 0.0026 $\text{ml O}_2 \cdot \text{ml}^{-1} \cdot \text{min}^{-1}$ for resting human skeletal muscle (3).

AZ, a CA inhibitor (31), 5-*N,N*-dimethylamiloride-hydrochloride (DMA), a specific inhibitor of NHE1 type Na^+/H^+ antiporters (48), and 4,4'-diisothiocyanostilbene-2,2'-disulphonate (DIDS), an inhibitor of anion channels, were obtained from Sigma.

Experimental procedure. Approximately 2.0 ml of myotubes in gelatin carriers or H-2K cells in agarose microcarriers suspended in perfusate solution were introduced into the NMR tube (see Fig. 2). This was done as rapidly as possible in order that the cells, which are grown under an oxygenated atmosphere, do not become anoxic during preparation of the experiment. The cells were perfused for 1.5–4 h to allow pH and PCr to stabilize (stabilization or control period), then the peristaltic pump was turned off for 2–3.5 h to expose them to anoxia, at the end of which time perfusion was restarted and maintained for 1–4 h to observe the chemical changes during recovery. In the experiments with AZ and DMA, the drug was added to the perfusion medium at the start of the experiment or at least 30 min before perfusion was halted. In the experiments with DIDS, because of its damaging effect on the cells, it was not added until after 1 h of stabilization.

The requirements of cells for oxygen are critical. Although the perfusate contains a PO_2 of >350 Torr, diffusion to the center of a volume that is consuming O_2 can require large oxygen gradients, as was pointed out by Krogh (25). The magnitude of this change in (Δ) PO_2 to the center of the sphere can be computed from Eq. 1.

$$\Delta\text{PO}_2 = aR^2/6D \quad (1)$$

where a is the average O_2 consumption in the sphere (in $\text{ml O}_2 \cdot \text{ml volume}^{-1} \cdot \text{min}^{-1}$), R is the radius of the sphere (in cm), and D is the diffusion coefficient of O_2 in saline, 1.2×10^{-8} $\text{ml} \cdot \text{min}^{-1} \cdot \text{Torr}^{-1} \cdot \text{cm}^{-1} \cdot \text{area}$ (in cm^2) $^{-1}$ (10). ΔPO_2 for an H-2K cell with an O_2 consumption of 0.006 $\text{ml} \cdot \text{ml}^{-1} \cdot \text{min}^{-1}$ and a radius of 5.4 μm is only 0.024 Torr, a negligible fraction of 350 Torr. Myotubes on the surface of the gelatin beads have a thickness of ~ 5 μm , so the ΔPO_2 in them will also be negligible. There must be an even thinner stagnant layer of perfusate with no O_2 consumption on the surface of the myotubes, which can be neglected. However, the agarose beads have a diameter of 0.028 cm (Fig. 1) and are 35% H-2K cells, so the average O_2 consumption in the bead volume is 0.0022 $\text{ml} \cdot \text{ml}^{-1} \cdot \text{min}^{-1}$. The calculated ΔPO_2 into their center is 23 Torr, which leaves a more than adequate PO_2 in the center of the beads. The need of the perfused cells for substrate is more than satisfied by the 25 mM of glucose in the perfusate. Allowing for the dilution of cells by perfusate in the NMR tube, all of the dissolved O_2 would have been consumed in <1 min after perfusion stopped, and anaerobic metabolism would have begun.

To test the health of the cells experimentally, pH and the phosphate metabolites of the myotubes and the H-2K cells were monitored by NMR with and without 0.1 or 10 mM AZ for up to 7.5 h in the perfusion setup, a total of four experiments. The cells remained

metabolically healthy, as judged by pH and PCr, which were steady after an initial period of stabilization. In three experiments on H-2K cells, they actually underwent two cycles of perfusion, no perfusion, and reperfusion for a total of >15 h, at the end of which pH and PCr were at the control levels. We, therefore, conclude that our preparation maintains the cells viable and healthy for the duration of our experiments.

To increase the signal-to-noise ratio, 400–800 spectra were collected over 10–20 min and summed for each data point, which multiplied the size of the peaks proportionally while the noise largely canceled because it was random. The collection intervals used were the shortest that gave a satisfactory ratio of signal to noise. In interpreting the data, it should be noted that complete recovery of pH within 20 min, for instance, implies recovery within a shorter interval. If recovery were $\geq 90\%$, for instance, then there could have been a delay of no more than 2 min.

Statistical analysis. To estimate the probability that a difference between a control and an experimental outcome was due to chance, Fisher's exact probability test for a 2×2 table was used (9). For data consisting of small samples, this test is more precise than is a test designed for large samples. For a full description of the test, see <http://faculty.vassar.edu/lowry/fisher.html>. The significance of a difference between values in the tables was determined by *t*-test, assuming the data varied as a normal distribution.

RESULTS

We carried out 26 successful cell experiments, 9 on rabbit neonatal myotubes on gelatin beads and 17 on the H-2K cells in agarose beads, and were able to obtain well-defined NMR peaks of PCr, P_i , and β -ATP with a collection time of 10 min, although, in some experiments, it was necessary to collect for 20 min. An example of neonatal rabbit myotube spectra during 2.5–3 h of stabilization, 1.5 h with no perfusion ("anoxia"), followed by reperfusion, is given in Fig. 3.

Representative graphs of the time course of pH during an experimental cycle in neonatal rabbit myotubes are presented in Fig. 4 and in H-2K cells in Fig. 5. Cell pH fell within the first 10 min after perfusion stopped. The abrupt fall of ~ 0.5 unit in the first time period appeared in 4 of 7 experiments on both types of cells without AZ and in none of 10 experiments with AZ ($P = 0.015$), suggesting an immediate inhibitory action of AZ. The pH continued to fall in a concave upward fashion during the rest of the anoxic period and in the absence of AZ began to rise immediately, that is, within 10 min, after the start of reperfusion (Figs. 4A and 5A). pH recovery began within the first measurement period after the start of reperfusion and was complete within a collection period. Average values for pH in the control, anoxic, and reperfusion periods and the average rate of fall of pH are given in Table 1. The pH values during the control and recovery periods were 0.1–0.2 pH units higher than reported in the literature (2), presumably because the extracellular pH was 7.5, compared with the value of 7.4 in normal animals, and the HCO_3^- was 35.5 mM, 40% higher than the normal value of 25 mM. The pH values for H-2K cells were more variable than those of the neonatal rabbit myotubes.

Effect of AZ on pH. Representative time courses of rabbit and H-2K myotube pH during a cycle in the presence of AZ are presented in Figs. 4B and 5B. In the presence of AZ, cell pH fell during the anoxic period similarly to the experiments in the absence of AZ. pH during the three experimental periods and the average rates of pH fall during anoxia were not different from those in the control experiments (Table 1). However, pH recovery was inhibited, and its onset was delayed 20 min in

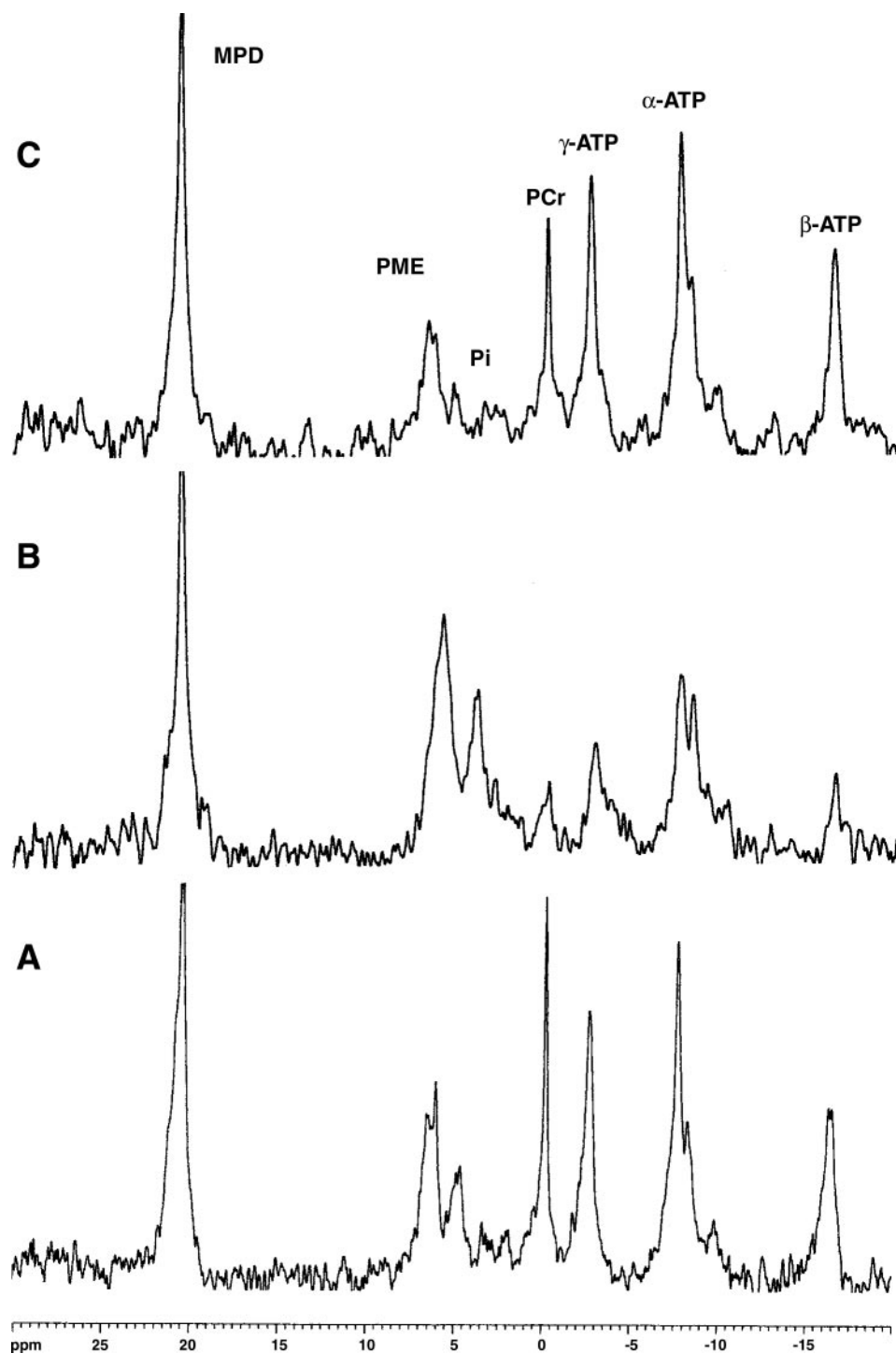


Fig. 3. ^{31}P -NMR spectra of neonatal myotubes growing on cross-linked gelatin beads during the control period (A), at the end of anoxia (B), and during recovery (C), plotted against the magnetic field strength in parts per million (ppm). MDP, methylene diphosphonic acid (standard); PME, phosphomonoester; PDE, phosphodiester; PCr, phosphocreatine. γ , α , and β are phosphate groups of ATP.

rabbit myotubes (Fig. 4B) and 40 min in H-2K cells (Fig. 5B). Once pH recovery started, the rate of rise was as rapid as it was in the absence of AZ; it returned to control levels within the next collection period and remained there for the duration of reperfusion. In 4 out of 10 experiments, pH overshoot the control values in the presence of AZ, including both neonatal myotubes and H-2K cells. No useful estimate of the rate of pH recovery can be calculated, only a lower limit, which was essentially the same for all experiments and therefore is not

included in Table 1. The time course of recovery did not correlate consistently with different durations of anoxia.

By treating the delay in onset of pH recovery as an event that occurred or did not occur, the probability that the delay in pH recovery in the presence of AZ was random was 0.029 for neonatal rabbit myotubes and 0.008 for H-2K cells. It is important to note that perfusion was always turned off or on within <1 min after a spectrum had been collected, as indicated by a data point, and the extracellular fluid was entirely

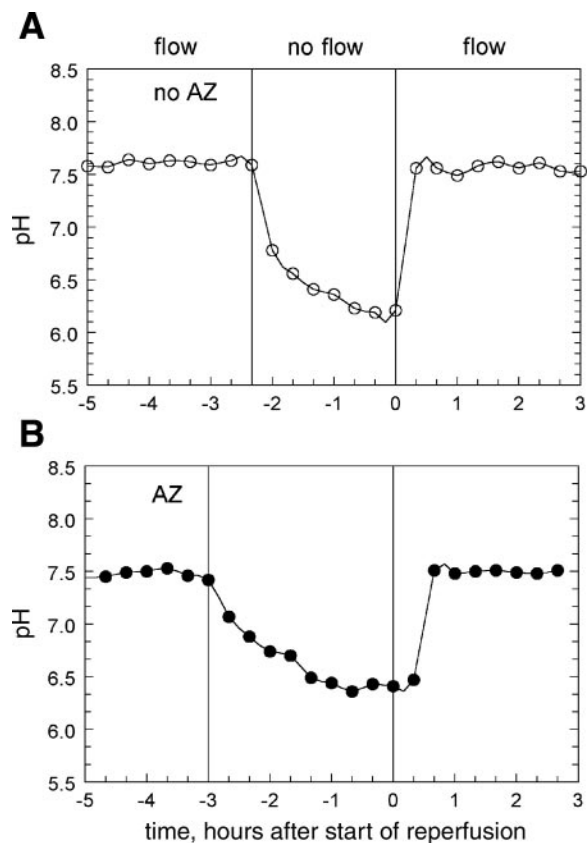


Fig. 4. Intracellular pH obtained by ³¹P-NMR in neonatal rabbit myotubes vs. time in hours, through a stabilization (control) period, an anoxic period, and a final period of reperfusion. Time zero indicates the start of reperfusion: A: no acetazolamide (AZ) in perfusate; B: 0.1 mM AZ in perfusate throughout.

replaced by fresh perfusate in 4 min. Thus a delay of one time point (≥ 10 min) on the graph is significant.

The intracellular pH fell from 7.4–7.5 to a nadir, at the end of a period of ischemia, of 6.24–6.44 in neonatal rabbit myotubes and 6.25–6.69 in H-2K cells. Nielsen (34) reported that arm venous blood pH in Olympic oarsmen can drop to 6.74 with a high lactate concentration, and the pH in the working muscles must have been much lower. The pH in the electrically stimulated leg muscles of a rabbit can decrease to 6.2 (47). Thus the pH in these cell preparations at the end of a period with no superfusion was similar to that in skeletal muscle *in vivo* at the end of heavy exercise.

Effect of AZ on phosphorus metabolites. Representative time courses of PCr during an experimental cycle in neonatal rabbit myotubes without and with AZ are presented in Fig. 6, and for H-2K cells, in Fig. 7. PCr concentrations during control, anoxia, and reperfusion periods are given in Table 2. Its values varied widely because of differences in the amount of creatine uptake by the cells. A similar wide variation in initial P_i also occurred (Table 3). PCr fell during the anoxic period in a more linear curve than pH in all experiments, reaching zero in two out of three experiments on myotubes without AZ and in two out of four experiments with AZ, but in no experiments with H-2K cells. The initial, control PCr in the rabbit myotubes was approximately three times greater than the similar values in H-2K cells, and the rate of fall was also greater (significant of both at $P < 0.01$), but the fractional decrease in PCr at the

nadir was not significantly different in the two types of cells. PCr did not recover to the control level during reperfusion. A delay in the onset of PCr recovery occurred in every experiment in the presence of AZ but in none in its absence, an effect significant at the $P = 0.03$ level.

Representative graphs for the time courses of P_i without and with AZ in experiments on rabbit myotubes and H-2K cells are presented in Figs. 8 and 9, respectively; the data are given in Table 3. P_i rose during anoxia and, in the absence of AZ, fell to control levels within one observation period after the start of reperfusion in all seven experiments. In the presence of AZ, the initiation of the fall in P_i was delayed in four out of four experiments on myotubes and in five out of five experiments on H-2K cells. The probability that the delay in recovery was random was 0.028 and 0.008, respectively.

Total cell phosphate (TP) includes PCr, P_i, ATP, sugar phosphates, and other compounds and provides an index of the number of living cells at any time during the experiment. The organic phosphates, which make up the majority of TP, do not permeate intact cell membranes but can leak out when the cells die. During the period without superfusion, any phosphate that leaks out of the cells would still remain in the magnetic field, and therefore, would be included in the measured TP, and, therefore, would not correctly indicate surviving cell mass. However, as soon as the phosphate-free superfusate flow resumes, any extracellular phosphate would be washed away, and TP would represent living cells. Generally, TP drifted downward slightly over the total experimental duration, but in experiments with DIDS it

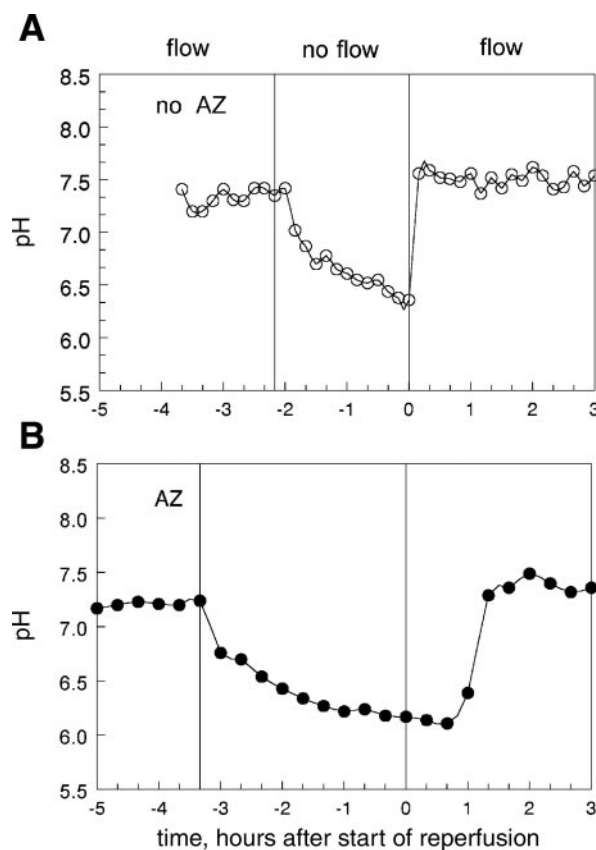


Fig. 5. Intracellular pH obtained by ³¹P-NMR in H-2K cells vs. time in hours as in Fig. 4. A: no AZ; B: with 0.1 mM AZ throughout.

Table 1. Effect of AZ and DMA on cell pH during anoxia and recovery

| | n | pH | | | Average Rate of Fall in pH, pH/min | Average Delay in Start of pH Rise, min | No. of Experiments with Delay Over Total No. of Experiments |
|------------|---|--------------|-----------|------------|------------------------------------|--|---|
| | | Start Anoxia | Nadir | Recovery | | | |
| Myotubes | | | | | | | |
| Control | 3 | 7.56±0.05 | 6.24±0.35 | 7.50±0 | 0.0078±0.0020 | 0 | 0/3 |
| AZ | 4 | 7.50±0.05 | 6.44±0.03 | 7.63±0.12 | 0.0069±0.0011 | 22.5±2.3 | 4/4 P=0.029 |
| H-2K cells | | | | | | | |
| Control | 4 | 7.39±0.17 | 6.52±0.26 | 7.64±0.05 | 0.0078±0.0014 | 0 | 0/4 |
| AZ | 5 | 7.44±0.11 | 6.69±0.15 | 7.46±0.05 | 0.0048±0.0012 | 23.3±8.6 | 5/5 P=0.008 |
| DMA | 3 | 7.26±0.04 | 6.08±0.01 | 6.83±0.185 | 0.020±0.002 | 16.7±3.3 | 3/3 P=0.029 |

Values are averages ± SE; n, no. of experiments. H-2K, H-2K^b-ts a58. Start anoxia, or end of stabilization, indicates the average value in the last 40 min of the control period, just before anoxia started. Nadir is the lowest value at the end of anoxia. Recovery indicates the plateau value after reperfusion started. There were no significant differences between the results, except for the last column, the occurrence or nonoccurrence of a delay in onset of the recovery of pH. The probability that the delay in recovery of pH with acetazolamide (AZ) and dimethylamiloride (DMA) was random is given in the last column.

decreased a large amount on reperfusion, suggesting reperfusion injury. Experiments in which the total phosphate fell immediately on reperfusion to less than one-fourth of its value at the end of anoxia were eliminated because most of the cells were considered to have died.

The ATP concentration, which was assumed to be 4.3 mM in the stabilized control period, did not demonstrate any consistent decrease in anoxia or delay in recovery related to the presence of AZ for either cell type. While in some experiments it declined with anoxia, in approximately an equal number of experiments it did not change. In those experiments in which

total phosphate fell sharply on reperfusion, indicating death of cells, ATP fell markedly.

Effect of DMA on pH and metabolic recovery. DMA, which specifically inhibits the Na⁺/H⁺ antiporter or NHE1 (at a concentration for half-maximal inhibition, K_i, of 0.3 μM) (48), was added in a concentration of 10 μM to the perfusate in three experiments on H-2K cells. Representative time courses for pH, PCr, and P_i in one experiment are graphed in Fig. 10, and the average data are given in Tables 1, 2, and 3, respectively.

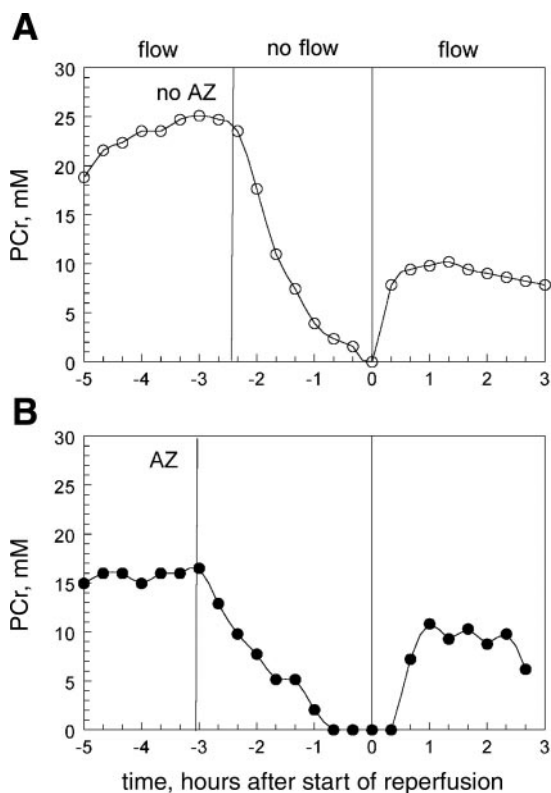


Fig. 6. Intracellular PCr obtained by ³¹P-NMR in myotubes vs. time in hours as in Fig. 4. A: no AZ; B: with 0.1 mM AZ throughout.

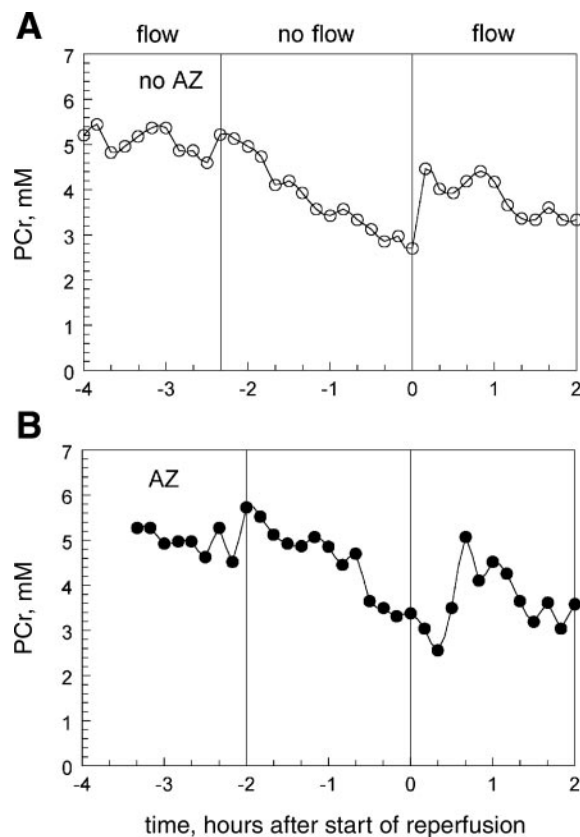


Fig. 7. PCr obtained by ³¹P-NMR in H-2K cells vs. time in hours as in Fig. 4. A: no AZ; B: with 0.1 mM AZ throughout.

Table 2. Effect of AZ and DMA on cell PCr during anoxia and recovery

| | n | PCr | | | Average Rate of Fall in PCr, mM/min | Average Delay in Start of PCr Rise, min | No. of Experiments with Delay over Total No. of Experiments |
|------------|---|---------------------|----------|-------------|-------------------------------------|---|---|
| | | Start of Anoxia, mM | Nadir, % | Recovery, % | | | |
| Myotubes | | | | | | | |
| Control | 3 | 27.4±1.8 | 9.3±9.3 | 59±13 | 0.147±0.022 | 0 | 0/3 |
| AZ | 4 | 25.0±4.3 | 8.0±5.1 | 64±2.2 | 0.14±0.0022 | 40±12 | 4/4 P=0.029 |
| H-2K cells | | | | | | | |
| Control | 4 | 7.1±1.8 | 44±4.3 | 76±7.6 | 0.036±0.011 | 0 | 0/4 |
| AZ | 3 | 8.3±1.6 | 32±14 | 27±12 | 0.030±0.010 | 13±6.7 | 3/3 P=0.029 |
| DMA | 3 | 9.0±2.2 | 33±15 | 68±16 | 0.107±0.050 | <80 | 3/3 P=0.029 |

Values are averages ± SE; n, no. of experiments. The column headings and numbers are explained in Table 1. Values at nadir and recovery are given in % of value at start of anoxia. Myotube phosphocreatine (PCr) is significantly greater than H-2K PCr; at the start of anoxia in the absence of AZ by $P=0.01$ and in the presence of AZ by $P=0.05$; in the recovery period in the absence of AZ by $P=0.05$ and in the presence of AZ by $P=0.01$. The probability that the delay in recovery of PCr in the presence of AZ was random is given in the last column.

The average pH values were the same as in other experiments, except that the nadir in H-2K cells with DMA was significantly lower than that in neonatal myotubes. The pH did not recover to the control level, and its rise after reperfusion was delayed in all three experiments (Table 1). The average rate constant for the fall in pH during anoxia was greater than for the control experiment, but this difference was only significant at the 0.05 level. PCr concentration was similar to control values throughout the cycle, as was the average rate constant for the decrease in PCr. The initial P_i was not different from that of the H-2K control data and fell to a similar minimal value during anoxia, and the start of its recovery after reperfusion was delayed in all three experiments, a significant difference at the $P = 0.03$ level. Thus DMA retarded the recovery of pH, PCr, and P_i after a period of anoxia.

Effect of DIDS on pH and metabolic recovery. In three experiments on H-2K cells, 0.200 mM DIDS was added to the perfusate, and the results of a representative experiment are graphed in Fig. 11. During the control period in all experiments, PCr, ATP, P_i , and pH were stable until perfusion stopped, at which time pH, PCr, and ATP began to fall and P_i to rise as in the other experiments, but PCr and ATP continued to fall, both through reperfusion and never recovering. In all

three experiments, P_i recovered, that is it fell, in two after and in one before reperfusion, but total phosphorus also fell, indicating cell death and washout of extracellular P_i . We concluded that DIDS damages the cells, which, combined with anoxia, causes their death, so their data are not included in the Tables 1–3.

Effect of AZ on cell lactate. We measured the relative cell lactate level during cycles of stabilization, anoxia, and reperfusion in two experiments on neonatal rabbit myotubes and two on H-2K cells, both with and without 0.1 mM AZ. (Fig. 12). There was no absolute standard, so the data are all normalized to 10 at zero time, i.e., when reperfusion began. Lactate began to rise immediately when anoxia started and increased 1.4- to 2.6-fold within 1 h. In none of the experiments had any value returned to overlap with its preanoxia range as long as observations continued, namely 1–3 h.

DISCUSSION

Cell pH. Aickin and Thomas (2) postulated two mechanisms for the removal of H^+ produced by the efflux of NH_3 from surface fibers of mouse soleus, the major one a Na^+/H^+ antiporter and a minor one involving HCO_3^- and CO_2 . A

Table 3. Effect of AZ and DMA on cell P_i during anoxia and recovery

| | n | P_i | | | Average Rate of Rise of P_i , mM/min | Average Delay, min | No. of Experiments with Delay Over Total No. of Experiments |
|------------|---|------------------|---------|-------------|--|--------------------|---|
| | | Start Anoxia, mM | Peak, % | Recovery, % | | | |
| Myotubes | | | | | | | |
| Control | 3 | 6.22±2.49 | 255±55 | 111±31 | 0.049±0.013 | 0 | |
| AZ | 3 | 6.11±1.34 | 310±126 | 246±160 | 0.045±0.015 | 17.5±4.9 | |
| | | | | | | 3/3 P=0.05 | |
| H-2K cells | | | | | | | |
| Control | 4 | 3.16±0.59 | 190±19 | 65±4 | 0.023±0.004 | 0 | |
| AZ | 5 | 2.92±0.75 | 333±114 | 96±24 | 0.036±0.008 | 36±11.2 | |
| | | | | | | 5/5 P=0.008 | |
| DMA | 3 | 2.63±0.45 | 343±72 | 275±107 | 0.096±0.0084 | >80 | |
| | | | | | | 3/3 P=0.029 | |

Values are averages ± SE; n, no. of experiments. The column headings and numbers are explained in Table 1. Values at peak and recovery are given in % of value at start of anoxia. The probability that the delay in recovery of P_i in the presence of AZ or DMA was random is given in the last column. The rate of rise of P_i was significantly greater for myotubes than for H-2K cells at a probability level of 0.05. It was twice as large because the amount of PCr was twice as large in myotubes as in H-2K cells.

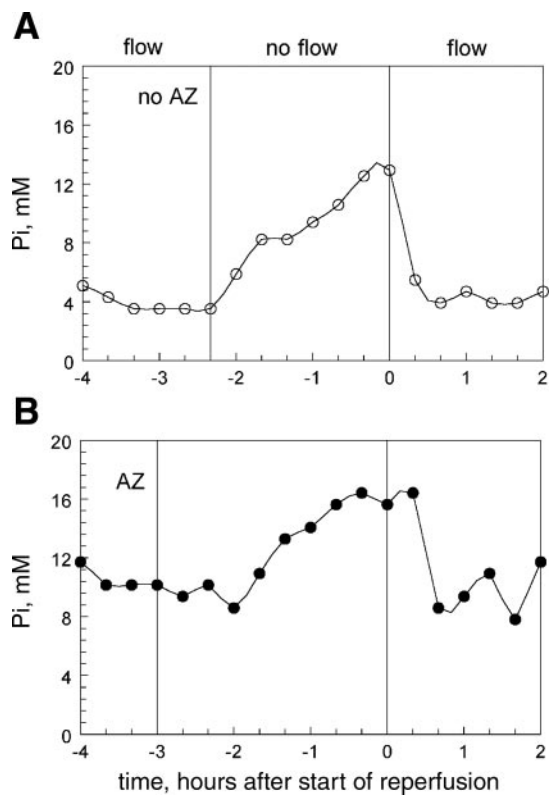


Fig. 8. P_i in myotubes vs. time in hours as in Fig. 4. A: no AZ; B: with 0.1 mM AZ throughout.

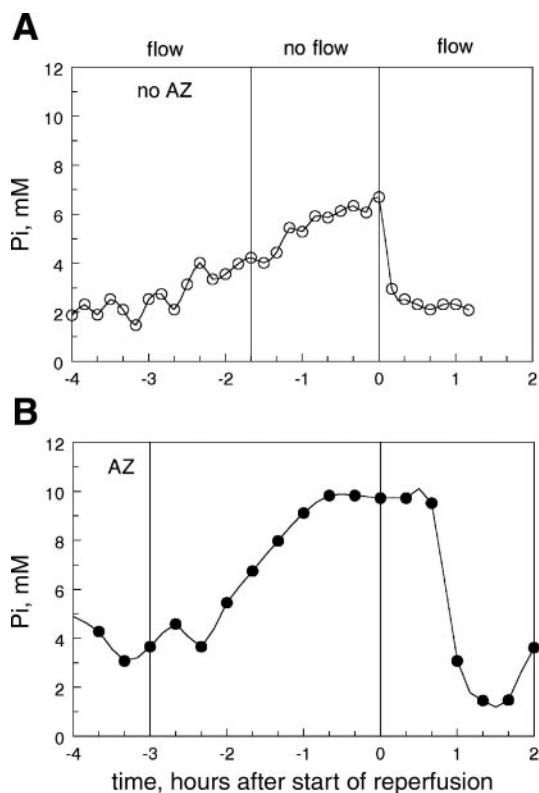


Fig. 9. P_i in H-2K cells vs. time in hours as in Fig. 4. A: no AZ; B: with 0.1 mM AZ throughout.

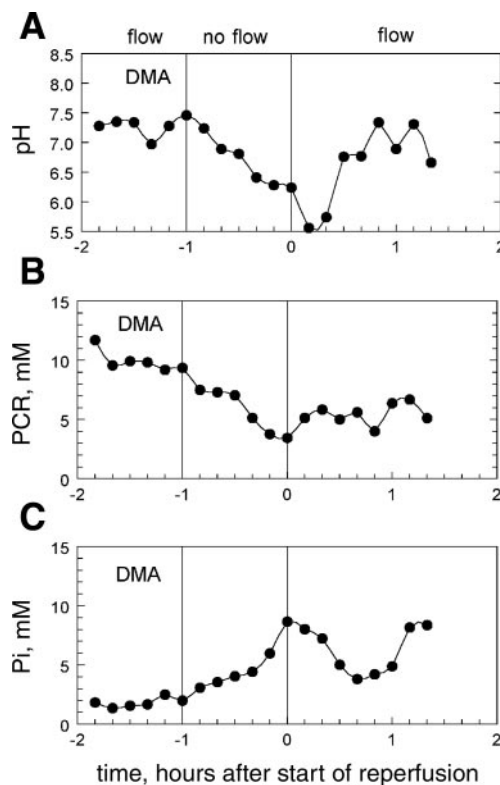


Fig. 10. pH (A), PCr (B), and P_i (C) in H-2K cells in the presence of 10 μ M dimethylamiloride (DMA) against time in hours, including the stabilization period. Results in the absence of DMA for pH, PCr, and P_i are shown in Figs. 4A, 6A, and 8A, respectively.

lactate-proton cotransporter has been proposed as a third mechanism to eliminate protons from skeletal muscle (22, 49, 50).

The Na^+/H^+ antiporter (39) is a family of ubiquitous stoichiometric transporters, present in skeletal muscle (20), electrically neutral, requiring no ATP, but driven by the net force of the gradients of Na^+ and H^+ and inhibited by amiloride compounds. In the presence of DMA, a specific inhibitor (6) of the ubiquitous neutral Na^+/H^+ exchanger (NHE1), the initial

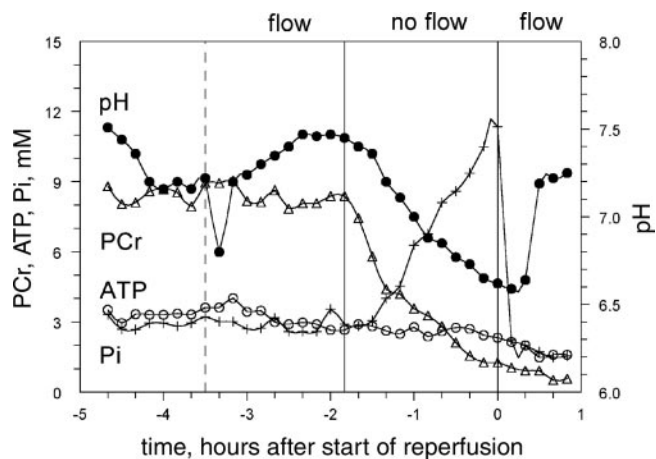


Fig. 11. pH and PCr, and ATP and P_i in mM against time in hours for H-2K cells during stabilization, anoxia, and reperfusion with the standard perfusate, to which was added 0.2 mM DIDS. The results are typical of 3 experiments. The dashed line shows the time of addition of DIDS.

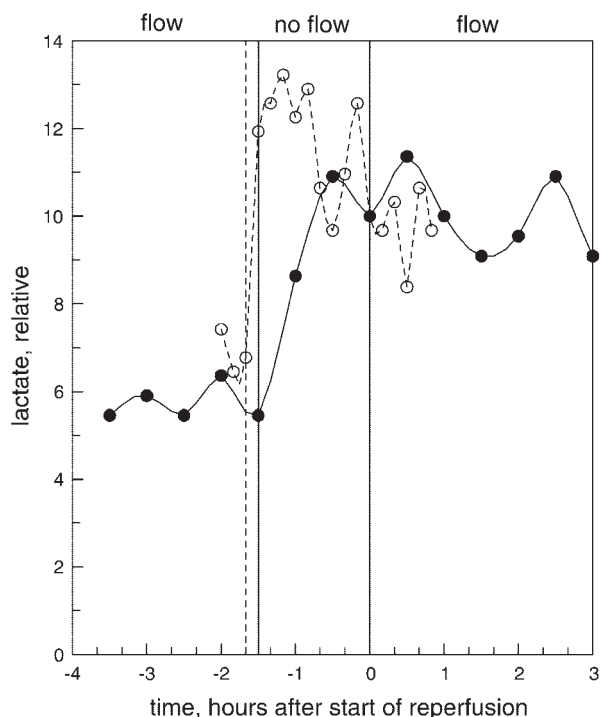


Fig. 12. Relative amount of lactate against time in hours for H-2K cells without AZ (dashed lines and open circles) and with 0.1 mM AZ (solid lines and solid circles). The vertical line at zero is the start of reperfusion, and lactate points are normalized to this value. Graphs of myocytes with and without AZ were similar.

recovery of pH after anoxia was completely inhibited (Fig. 10). Amiloride also delays the recovery of pH from exercise in rat calf muscle (6). The activity of this antiporter has been reported to decrease when ATP is depleted, but further investigation showed that this is not caused by the reduction in ATP per se, but possibly by phosphorylation of other molecules (1). In our experiments, ATP levels varied $\pm 30\%$ from point to point, but the average remained constant through anoxia in one-half of the experiments, and fell in one-half, in several to zero. However, there was no correlation with pH or metabolic recovery. We conclude that the Na^+/H^+ antiporter participates in the recovery of pH in our experiments.

In the second mechanism of acid export, the CO_2 mechanism, studied in erythrocytes, HCO_3^- enters the muscle cell in exchange for another anion (41), probably chloride, and reacts to form CO_2 , which diffuses out of the cell, completing a proton transfer across the impermeable membrane of the erythrocyte. This was first described by Jacobs and Stewart (18). Aickin and Thomas (2) found that DIDS, which blocks the rate of HCO_3^- entrance into the cells, reduced the rate of proton removal from mouse soleus cells rendered acid by NH_3 removal. They did not inhibit CA or subject the cells to anoxia. CA II in the cytoplasm would accelerate the formation of CO_2 , although the half time of the uncatalyzed reaction is ~ 5 s (17), rapid enough to complete the release of the gas in 10 min, the spectra collection period for the present experiments.

It is most probable that the main action of AZ is to block the NHE1 antiporter for the following reasons. 1) The export of protons by the CO_2 mechanism is small compared with that of the antiporter, as noted by Aickin and Thomas (2). 2) AZ

blocked the recovery of pH to the same extent as DMA, which is presumably inhibiting only the Na^+/H^+ antiporter. 3) During the lag period after reperfusion produced by both DMA and AZ, there is a large inward gradient of HCO_3^- , which might be expected to move the anion into the cell, where it would form CO_2 and raise pH, which did not occur. We interpret this as presumptive evidence that the skeletal muscle cells are impermeable to HCO_3^- at this point. There may also be inhibition of the CO_2 transporter (11, 44), so the gas does not leave the cells easily.

It has been recognized for over 40 yr that the concentration of CA in mammalian red blood cells was several orders of magnitude greater than necessary to catalyze the exchange of CO_2 in the pulmonary capillaries (30, 31). The concentration of AE1 transporters approximates this excess concentration of enzyme (45). Thus it has become apparent that most of the CA II in the red blood cell is bound to the $\text{HCO}_3^-/\text{Cl}^-$ exchangers to enhance their activity, but not to accelerate the exchange of CO_2 per se between erythrocyte cytoplasm and plasma (40).

A lactate-proton cotransporter has been demonstrated in skeletal muscle (22, 49, 50) and proposed as a third mechanism for the removal of H^+ from muscle (21). However, although cell lactate concentration rose during anoxia, it did not fall during several hours of reperfusion (Fig. 11). Therefore, it could not have contributed significantly to the recovery of pH by any pathway. Biopsies of human skeletal muscle, after repeated 0.5-min bursts of exercise followed by 4-min rest periods, demonstrated similar increases in lactate concentrations, which fell during the first two rest periods but actually rose during the third (29). Our cells were stressed for a much longer period but did no work and, therefore, would be expected to metabolize less lactate. Garcia et al. (12) cloned a monocarboxylate transporter resembling the erythrocyte lactate transporter but found it restricted to mitochondria-rich skeletal muscle. The neonatal rabbit myotubes without calcium are reported to be mainly glycolytic (26), unless calcium is added to the growth medium, which suggests that a lactate transporter may not be present in our cells. Whole blood outside the cells, which may facilitate lactate export from skeletal muscle in vivo, is lacking in our preparation.

Function of CA in muscle. The only reported reaction of AZ is to inhibit CA, with the exception of competing with paraminobutyric acid in bacterial metabolism (14). Therefore, the effect of AZ in retarding pH recovery is expected to depend ultimately on its reaction with CA, or on some as yet unidentified reaction. The K_i values of the high-activity isozymes, CA II, CA IV, and CA V, for AZ are ~ 0.02 μM (42). The drug in the perfusate would have entered the cells within several minutes (17) and, at the concentrations used, 0.1 or 10 mM, would have inhibited all of the isozymes of CA within the cytoplasm and on the outer surface of the sarcoplasm, except CA III. This last isozyme has a low activity, a K_i for AZ of 0.306 mM, but is present only in slow-oxidative skeletal muscle, and the neonatal rabbit myotubes and H-2K cells are predominantly glycolytic. CA III has recently been shown to act as an antioxidant in skeletal muscle (51). Maren (30) found that increasing levels of AZ had no additional effect in animals, once CA was completely inhibited. A concentration of 0.1 mM is 5,000 times K_i , so 10 mM would not be expected to have any additional actions. Six pH experiments were carried out in 10 mM AZ and four in 0.1 mM AZ, but no significant differences

were observed in any of the data in the Tables 1–3. Inhibition of CA in the cell by AZ would slow the rate of CO₂ formation, which might then retard the rise in cell pH, but the uncatalyzed rate could complete the process by the next spectrum. It is not clear how a reduction of the rate of formation of CO₂ in the cytoplasm would cause a delay or lag in pH recovery. We did not use a membrane-impermeable CA inhibitor to separate the function of CA IV on the cell surface from that of isozymes inside the cell.

Because AZ is a specific inhibitor of CA and its acceleration of the reversible reactions of CO₂ appears of minimal importance in eliminating acid from the cells, AZ must be acting with CA in some other way. Li et al. (28) have shown that CA II binds to the intracellular COOH terminal of the Na⁺/H⁺ exchanger (NHE1) in vitro and increases the transport of H⁺ in a transfected Chinese hamster ovary cell line (AP1) containing human CA II and NHE1. AZ reduces the rate of this proton transport, presumably by binding to the CA attached to the NHE1 (a metabolon). CA binds to the cytoplasmic chain of the band III protein (AE1) in red blood cells, and its inhibition interferes with anion movement (40, 45, 46), analogous to its effect on the Na⁺/H⁺ antiporter. This raises the possibility that, by an analogous mechanism, AZ reduces HCO₃⁻ entrance into skeletal muscle cells by anion exchange and thus lowers the export of protons by the CO₂ mechanism. The K_i for the inhibition of the AZ-sensitive fraction of anion transport is reported as 54 μM (45), some 2,700 times the K_i for the catalytic action of CA II (4, 17, 17). Thus 0.1 mM AZ would still inhibit ~67% of the sulfonamide-sensitive AE1 anion transport. The CA activity and the enzyme inhibition constant for ethoxolamide, a lipid-soluble high-affinity CA inhibitor, are the same in human red blood cells as in the lysate (4, 17). Therefore, the binding of CA II to AE1 and NHE1 does not affect the active site of the CA.

Our experiments showed that AZ delayed recovery of pH for 10–30 min, during which period neither NHE1 nor AE1 was working effectively, temporarily inhibited by the sulfonamide. Investigation of the mechanism of disinhibition after the delay requires further work. Kowalchuk et al. (24) found a 6-min delay in the recovery of pH after exercise in the human forearm in the presence of AZ, but the rate of rise in pH was the same as in the absence of the drug, analogous to Figs. 4B and 5B.

PCr and P_i recovery. Kowalchuk et al. (24) did not report absolute concentrations of PCr and P_i, only P_i/PCr, but this ratio should have shown a delay in recovery if PCr and/or P_i were delayed, but it did not. PCr fell to zero during anoxia in four experiments with our neonatal rabbit myotubes, while Kowalchuk et al. did not report large values of P_i/PCr, suggesting that the anoxic stress on our muscle cells was more severe.

There is no reported reaction by which AZ or DMA can inhibit directly the recovery of PCr from anoxia. PCr is replenished from ATP and creatine by the creatine kinase reaction, which is continuously in equilibrium on a physiological time scale as measured by ³¹P-NMR (35). Ponticos et al. (38) have shown that increased levels of AMP activate a kinase that phosphorylates creatine kinase and inhibits it. However, it presumably does not slow the enzyme enough to rate limit its function as an ATP buffer. We propose that the increased H⁺ in anoxia acts through the creatine kinase equilibrium to depress regeneration of PCr.

$$166 \times 10^7 = \frac{[\text{ATP}][\text{Creatine}]}{[\text{ADP}][\text{PCr}][\text{H}^+]} \quad (2)$$

where brackets denote concentration. This argument implies that pH recovery has to take place before the recovery of PCr. In support of this, in no experiment was PCr or P_i recovery delayed, unless pH recovery was also delayed. We expect that pH increases before PCr, but, with the time resolution of our method, it is only possible to conclude that they have both recovered in 10 min.

P_i increases during anoxia because the ATP is dephosphorylated for metabolic needs, and the resulting ADP is phosphorylated by PCr with a net release of P_i. Sugar phosphates also break down, but we did not routinely measure them. With reperfusion and the end of anoxia, oxidative metabolism restarts and a steady-state value of ATP/ADP should be rapidly established. The ATP supplies metabolic needs and phosphorylates creatine. In the control experiments, this process was complete within 10 min, but, in the presence of DMA and AZ, no PCr was formed for 10 min or more. It is possible that the drugs prevent the initiation of oxidative metabolism, despite the high P_{O2}. For example, AZ might inhibit mitochondrial CA (CA V) and reduce metabolism of pyruvate (36), the major substrate. If this were the case, glycolysis would be needed to provide metabolic energy, and the pH would drop farther. However, it remained constant for the duration of the lag (Figs. 4 and 5).

In conclusion, protons are removed from skeletal muscle cells after acidosis produced by a period of anoxia almost entirely by a Na⁺/H⁺ antiporter. HCO₃⁻/anion exchange into the cells with formation of CO₂ and lactate-H⁺ cotransport contribute minimally. CA plays a significant role in regulation of cytoplasmic pH in skeletal muscle cells because AZ, a specific inhibitor of it, delayed recovery to normal pH from acidosis induced by anoxia, cessation of perfusion. This delay may not be due to inhibition of the CA activity itself but to a regulatory action of the enzyme on ion transport systems, the proton-sodium transporter and/or the HCO₃⁻/Cl⁻ exchanger. The delay in recovery of pH also delayed recovery of PCr and P_i to control levels. In vivo, AZ retards removal of acid from exercised skeletal muscle. We conclude that a major cause of this effect is inhibition of skeletal muscle CA itself rather than inhibition of erythrocyte CA.

ACKNOWLEDGMENTS

The authors owe deep thanks to Zhang Yong Wei and Ping Wang for excellent technical assistance, to Dr. T. A. Partridge for supplying the H-2K^b-ts A58 mouse soleus line, to Dr. Mary Selak for O₂ consumption measurements, to Dr. Martin Pring for help in statistics, and to Drs. Bayard Storey and Richard L. Veech for advice.

GRANTS

This research was supported by National Institute of Arthritis and Musculoskeletal and Skin Diseases Grant RO1 AR-045394.

REFERENCES

- Aharonovitz O, Demareux N, Woodside M, and Grinstein S. ATP dependence is not an intrinsic property of Na⁺/H⁺ exchanger NHE1: requirement for an ancillary factor. *Am J Physiol Cell Physiol* 276: C1303–C1311, 1999.
- Aickin CC and Thomas RC. Micro-electrode measurement of the intracellular pH and buffering power of mouse soleus muscle fibres. *J Physiol* 267: 781–810, 1977.

3. **Barcroft J and Dornhorst AC.** The blood flow through the human calf during rhythmic exercise. *J Physiol* 109: 402–411, 1949.
4. **Barinov I, Dodgson SJ, Forster RE, Itada N, and Lin L.** Graded inhibition of intracellular carbonic anhydrase activity in human red blood cells. *J Physiol* 371: 159P, 1985.
5. **Bental M, Pick U, Avron M, and Degani H.** Metabolic studies with NMR spectroscopy of the alga *Dunaliella salina* trapped within agarose beads. *Eur J Biochem* 188: 111–116, 1990.
6. **Counillon L, Touret N, Bidet M, Peterson-Yantorno K, Coca-Prados M, Stuart-Tilley A, Wilhelm S, Alper SL, and Civan MM.** Na⁺/H⁺ and Cl⁻/HCO₃⁻-antiporters of bovine pigmented ciliary epithelial cells. *Pflügers Arch* 440: 667–678, 2000.
7. **Daly MM and Seifter S.** Uptake of creatine by cultured cells. *Arch Biochem Biophys* 203: 317–324, 1980.
8. **Doliba NM, Wehrli SL, Babsky AM, Doliba NM, and Osbakken MD.** Encapsulation and perfusion of mitochondria in agarose beads for functional studies with 31-P NMR. *Magn Reson Med* 39: 679–684, 1998.
9. **Fisher RA.** *Statistical Methods for Research Workers.* Edinburgh: Oliver and Boyd, 1958.
10. **Forster RE.** Factors affecting the rate of exchange of O₂ between blood and tissues. In: *Oxygen in the Animal Organism.* New York: Pergamon, 1964, p. 393–409.
11. **Forster RE, Gros G, Lin L, Ono Y, and Wunder M.** The effect of 4,4'-stilbene-2,2'-disulfonate on CO₂ permeability of the red blood cell membrane. *Proc Natl Acad Sci USA* 95: 15815–15820, 1998.
12. **Garcia CK, Goldstein JL, Pathak RK, Anderson RG, and Brown MS.** Molecular characterization of a membrane transporter for lactate, pyruvate, and other monocarboxylates: implications for the Cori Cycle. *Cell* 76: 865–873, 1994.
13. **Geers C, Krüger D, Siffert W, Schmid A, Bruns W, and Gros G.** Carbonic anhydrase in skeletal and cardiac muscle from rabbit and rat. *Biochem J* 282: 165–171, 1992.
14. **Gilman AG, Goodman AS, and Gilman A.** *The Pharmacological Basis of Therapeutics.* New York: MacMillan, 1980.
15. **Henry RP.** Techniques for measuring carbonic anhydrase in vitro. In: *The Carbonic Anhydrases*, edited by Dodgson SJ, Tazshian RE, Gros G, and Carter ND. New York: Plenum, 1991, p. 119–125.
16. **Hsieh PS and Balaban RS.** ³¹P imaging of in vivo creatine kinase reaction rates. *J Magn Reson* 74: 574–579, 1987.
17. **Itada N and Forster RE.** Carbonic anhydrase activity in intact red blood cells measured with ¹⁸O exchange. *J Biol Chem* 252: 181–188, 1977.
18. **Jacobs MH and Stewart DR.** The role of carbonic anhydrase in certain ion exchanges involving the erythrocyte. *J Gen Physiol* 25: 539–552, 1942.
19. **Jouvensal L, Carlier PG, and Bloch G.** Low visibility lactate in exercised rat muscle using double quantum proton spectroscopy. *Magn Reson Med* 38: 706–711, 1997.
20. **Juel C.** Intracellular pH recovery and lactate efflux in mouse soleus muscles stimulated in vitro: the involvement of the sodium/proton exchange and a lactate carrier. *Acta Physiol Scand* 132: 363–371, 1988.
21. **Juel C.** Lactate-proton cotransport in skeletal muscle. *Physiol Rev* 77: 321–358, 1997.
22. **Juel C, Kristiansen S, Pilegaard H, Wojtaszewski J, and Richter EA.** Kinetics of lactate transport in sarcolemmal giant vesicles obtained from human skeletal muscle. *J Appl Physiol* 76: 1031–1036, 1994.
23. **Kemp JG, Taylor DJ, and Radda G.** Control of phosphocreatine resynthesis during recovery from exercise in human skeletal muscle. *NMR Biomed* 6: 66–72, 1993.
24. **Kowalchuk JM, Shelly AM, Weening BS, Marsh GD, and Paterson DH.** Forearm muscle metabolism studied using ³¹P-MRS during progressive exercise to fatigue after Acz administration. *J Appl Physiol* 89: 200–209, 2000.
25. **Krogh A.** The number and distribution of capillaries in muscles with calculations of the oxygen pressure head necessary for supplying the tissue. *J Physiol* 52: 409–415, 1919.
26. **Kubis HP, Haller EA, Wetzel P, and Gros G.** Adult fast myosin pattern and Ca²⁺-induced slow myosin pattern in primary skeletal muscle culture. *Proc Natl Acad Sci USA* 94: 4205–4210, 1997.
27. **Lawson JW and Veech RL.** Effects of pH and free Mg²⁺ on the K_{eq} of the creatine kinase reaction and other phosphate hydrolyses and phosphate transfer reactions. *J Biol Chem* 254: 6528–6537, 1979.
28. **Li X, Alvarez B, Casey JR, Reithmeier RAF, and Fliegel L.** Carbonic anhydrase II binds to and enhances activity of the Na⁺/H⁺ exchanger. *J Biol Chem* 277: 36085–36091, 2002.
29. **Lindinger MI, McKelvie RS, and Heigenhaue GJ.** K⁺ and Lac⁻ distribution in humans during and after high-intensity exercise: role in muscle fatigue attenuation? *J Appl Physiol* 78: 765–777, 1995.
30. **Maren TH.** Carbonic anhydrase; chemistry, physiology and inhibition. *Physiol Rev* 47: 595–781, 1967.
31. **Maren TH.** The links among biochemistry, physiology and pharmacology in carbonic anhydrase mediated systems. In: *Carbonic Anhydrase. From Biochemistry and Genetics to Physiology and Clinical Medicine: Proceedings of the International Workshop on Carbonic Anhydrase, Held in Spoleto, Italy in March 1990*, edited by Botrè F, Gros G, and Storey BT. New York: VCH, 1991, p. 186–207.
32. **Morgan JE, Beauchamp JR, Pagel CN, Peckham CN, Ataliotis P, Jat PS, Noble MD, Farmer K, and Partridge TA.** Myogenic cell lines derived from transgenic mice carrying a thermolabile T antigen: a model system for the derivation of tissue-specific and mutation-specific cell lines. *Dev Biol* 162: 486–498, 1994.
33. **Neeman M, Rushkin R, Kadouri A, and Degani H.** Adaptation of culture methods for NMR studies of anchorage-dependent cells. *Magn Reson Med* 7: 236–249, 1988.
34. **Nielsen HB.** pH after competitive rowing: the lower physiological range. *Acta Physiol Scand* 165: 113–114, 1990.
35. **Nioka S, Argov Z, Dobson GP, Forster RE, Subramanian HV, Veech RL, and Chance B.** Substrate regulation of mitochondrial oxidative phosphorylation in hypercapnic rabbit muscle. *J Appl Physiol* 72: 521–528, 1996.
36. **Ono Y, Lin L, Storey BT, Taguchi Y, Dodgson SJ, and Forster RE.** Continuous measurement of ¹³C¹⁶O₂ production from [¹³C]pyruvate by intact liver mitochondria: effect of HCO₃⁻. *Am J Physiol Cell Physiol* 270: C98–C106, 1996.
37. **Osbakken MD, Wroblewski K, Zhang D, Ivanics T, and Wehrli S.** ³¹P relaxation rates to evaluate physiological events in the heart. *Magn Reson Med* 30: 498–502, 1993.
38. **Ponticos M, Lu QL, Morgan JE, Hardie DG, Partridge TA, and Carling D.** Dual regulation of the AMP-activated protein kinase provides a novel mechanism for the control of creatine kinase in skeletal muscle. *EMBO J* 17: 1688–1699, 1998.
39. **Putney LK, Denker SP, and Barber DL.** The changing face of Na⁺/H⁺ exchanger, NHE1: structure, regulation and cellular actions. *Annu Rev Pharmacol Toxicol* 42: 527–552, 2002.
40. **Reithmeier RA.** A membrane metabolon linking carbonic anhydrase with chloride/bicarbonate anion exchangers. *Blood Cells Mol Dis* 27: 85–89, 2001.
41. **Roos A and Boron WF.** Intracellular pH. *Physiol Rev* 61: 296–432, 1981.
42. **Sanyal G, Swenson ER, Pessah NI, and Maren TH.** The carbon dioxide hydration activity of skeletal muscle carbonic anhydrase. Inhibition by sulfonamides and anions. *Mol Pharmacol* 22: 211–220, 1982.
43. **Scott DP, Davidheiser S, and Coburn RF.** Effects of elevation of phosphocreatine on force and metabolism in rabbit aorta. *Am J Physiol Heart Circ Physiol* 253: H461–H465, 1987.
44. **Soupeine E, Inwood W, and Kustu S.** Lack of the Rhesus protein Rh1 impairs growth of the green alga *Chlamydomonas reinhardtii* at high CO₂ [see comment]. *Proc Natl Acad Sci USA* 101: 7787–7792, 2004.
45. **Sterling D, Reithmeier RA, and Casey JR.** A transport metabolon. Functional interaction of carbonic anhydrase II and chloride/bicarbonate exchangers. *J Biol Chem* 276: 47886–47894, 2001.
46. **Sterling D, Reithmeier RA, and Casey JR.** Carbonic anhydrase: in the driver's seat for bicarbonate transport. *JOP* 2: 165–170, 2001.
47. **Vandenborne K, McCully K, Kakihiro H, Prammer M, Bolinger L, Detre JA, De Meirler K, Walter G, Chance B, and Leigh JS.** Metabolic heterogeneity in human calf muscle during maximal exercise. *Proc Natl Acad Sci USA* 88: 5714–5718, 1991.
48. **Vigne P, Frelin C, Cragoe EJ Jr, and Lazdunski M.** Structure-activity relationships of amiloride and certain of its analogues in relation to the blockade of the Na⁺/H⁺ exchange system. *Mol Pharmacol* 25: 131–136, 1984.
49. **Von Grumbekow L.** Kinetics of lactate and pyruvate transport in cultured rat myotubes. *Biochim Biophys Acta* 1417: 267–275, 1999.
50. **Wetzel P, Hasse A, Papadopoulos S, Voipio S, Kaila K, and Gros G.** Extracellular carbonic anhydrase activity facilitates lactic acid transport in rat skeletal muscle fibres. *J Physiol* 531: 743–756, 2001.
51. **Zimmerman UJ, Wang P, Zhang X, Bogdanovich S, and Forster RE.** Anti-oxidative response of carbonic anhydrase III in skeletal muscle. *IUBMB Life* 56: 343–347, 2004.